

Multi-Fiber Reconstruction from DW-MRI using a Continuous Mixture of von Mises-Fisher Distributions *

Ritwik Kumar¹, Angelos Barmpoutis¹, Baba C. Vemuri¹, Paul R. Carney², Thomas H. Mareci³

¹ Department of Computer and Information Science and Engineering, University of Florida

² Department of Pediatrics, University of Florida

³ Department of Biochemistry and Molecular Biology, University of Florida

{rkkumar, abarmpou, vemuri}@cise.ufl.edu, carnepr@peds.ufl.edu, thmareci@ufl.edu

Abstract

In this paper we propose a method for reconstructing the Diffusion Weighted Magnetic Resonance (DW-MR) signal at each lattice point using a novel continuous mixture of von Mises-Fisher distribution functions. Unlike most existing methods, neither does this model assume a fixed functional form for the MR signal attenuation (e.g. 2nd or 4th order tensor) nor does it arbitrarily fix important mixture parameters like the number of components. We show that this continuous mixture has a closed form expression and leads to a linear system which can be easily solved. Through extensive experimentation with synthetic data we show that this technique outperforms various other state-of-the-art techniques in resolving fiber crossings. Finally, we demonstrate the effectiveness of this method using real DW-MRI data from rat brain and optic chiasm.

1. Introduction

Since the first publication of the derivation for the effect of a time-dependent magnetic field gradient on the spin-echo experiment by Stejskal and Tanner [30] in 1965 to measure the diffusional attenuation of the MR signal, numerous methods have been proposed to model the MR signal and the associated displacement probability. Much of this interest stems from the fact that even today, DW-MRI is the only non-invasive and in-vivo imaging method that allows examination of neural tissue architecture at a microscopic scale. By providing quantitative data suggestive of water molecule motion in brain tissue, DW-MRI has helped in elucidating white matter fiber directions (e.g. [19], [26]) and, through tractography, in inferring connectivity between brain regions (e.g. [38], [9], [22]).

*This research was supported in part by NIH EB007082 to BCV, NIH EB004752 to PC and TM and in part by the UF Alumni Fellowship to RK and AB.

The recovery of local (intra-voxel) fiber orientations generally involves three steps, first is the modeling of the MR signal, second is estimation of water displacement probability distribution function (PDF) from the signal via its fourier transform [26] and the third is the radial integral (or radial iso-surface computation) of the displacement probability function to obtain the fiber orientation distribution function (ODF), directions of whose maxima give the local fiber orientations. In the past, various models for fiber orientation recovery have been suggested which target different stages of this process. In this paper, we present a novel technique for fiber orientation recovery which uses a mixture of von Mises-Fisher distributions to model the MR signal attenuation. Before providing details of our model, we present a survey of the existing methods which attempt to solve the problem of fiber orientation recovery.

The Diffusion Tensor MRI (DT-MRI) model assumes the diffusivity function to be a rank 2 tensor and its displacement probability is characterized by an oriented Gaussian distribution. Though this model, which uses multi-directional DW-MRI data [8], has been effective in modeling regions with high white-matter coherence, it has the major limitation that it cannot cope with complex local fiber geometries and can only model a single fiber orientation at a voxel.

To overcome this limitation of the DTI model, High Angular Resolution Diffusion Imaging (HARDI) was proposed by Tuch [33]. This high resolution data allowed modeling of the the diffusivity function in Stejskal-Tanner mono-exponential signal attenuation model [30] using generalized high order Cartesian tensors ([25], [6]) and spherical harmonics expansion ([15], [2]). Though these methods are capable of handling more complex local geometry of the diffusivity function than DT-MRI, they do not necessarily yield the correct fiber orientations as the peaks of diffusivity function within a voxel does not necessarily align with the local fiber orientations [26].

This led to the development of model independent techniques which directly estimated fiber PDF (mentioned above as the stage two of the fiber orientation recovery process). In the Q-ball imaging (QBI) technique ODF is approximated by the spherical Funk-Radon transform ([34],[36]) and more recently using spherical harmonic basis for Funk-Radon transform ([4],[14][16]). The problem with these methods is that they only yield the displacement probability convolved with the zeroth order Bessel function. Diffusion spectrum imaging (DSI), which presents itself as an alternative to Q-ball suffers from time-intensive sampling requirements [37].

More recently, Ozarslan *et al.* [26] introduced diffusion orientation transform (DOT), by evaluating the radial part of the Fourier integral (mentioned as stage 2 in the general process) analytically. Their proposal suffers from the fact that the obtained displacement probability is corrupted by a convolution with a non-analytical function, unless a more data intensive bi-exponential model is used.

At a contrast to the models mentioned above are the multi-compartmental models, which attempt to model the MR signal or ODF as a mixture of some basis functions in order to resolve intra-voxel orientation heterogeneity (IVOH). Tuch *et al.* [35] used a finite mixture of Gaussian densities to estimate the diffusion signal. Similar attempts to resolve multiples fibers were presented in [5] and [10]. A finite mixture of von Mises-Fisher distributions (used in conjunction with DOT [26]) was presented in [24] for modeling ODF. These methods suffer from the two major problems. First, the number of components in the mixture is arbitrarily fixed (this is the all important model selection problem) and second, these methods use non-linear fitting methods to find the unknown parameters which can be unstable in the case of multiple fiber crossings (as the number of parameters increases).

To address the problems of multi-compartmental models, spherical deconvolution was applied by Tournier *et al.* [31], which assumes a distribution of fiber at each voxel. This method does not assume any fixed number of fiber orientations at each voxel and leads to linear systems which can be solved efficiently. Recently variants of this technique were proposed in [1], [4] and [32]. Bhalerao *et al.* [11] proposed a method for modeling HARDI data using a mixture of hyperspherical von Mises-Fisher distributions and employed EM algorithm for parameter estimation. They used Akaike information criterion for estimating the number of components in the mixture.

More recently, using the spherical deconvolution method and a mixture of Wishart distributions, Jian *et al.* [17], [19] showed that the MR signal is the Laplace transform of a continuous mixing distribution of diffusion tensor. Since each diffusion tensor is a positive definite matrix, the mixing distribution was chosen to be a mixture of Wishart dis-

tributions. The seminal contribution of this work was the analytical derivation of the Rigaut type asymptotic fractal expression [27] which so far, has only been fitted phenomenologically to the diffusion weighted MR data[20].

Our work presented in this paper uses a continuous mixture of von Mises-Fisher (vMF) distribution functions to estimate the MR signal. In this continuous mixture, we use a mixture of von Mises-Fisher as the mixing density. Once the signal has been modeled, we use the method proposed in [7] to recover the displacement probability (one can also use any of the other published methods) from which orientations of fibers are extracted by fixing the radius magnitude [36] (radial integration as proposed in [26] can also be used). In our mixture model we preserve the advantages that spherical deconvolution based methods have over multi-compartmental methods as in our method, neither the number of components be pre-decided nor any non-linear optimization technique be used to obtain the mixture weights. Further, as our method is based on direct discretization of S^2 , unlike [19], we do not need to make assumptions to transform the discretization problem from \mathcal{P}_3 to S^2 .

The rest of the paper is organized as follows. In Sec. 2 we describe our framework for modeling the MR signal and recovering fiber orientations from it. In Sec. 3 extensive experimental results are presented, and in Sec. 4 we conclude with a summary of our contribution.

2. Theory

Since we seek a probabilistic model for the MR signal, which is defined over a sphere, S^2 , use of a distribution which is defined over this domain is natural. Of the various distributions defined on a sphere, we picked von Mises-Fisher because it is the analog of Gaussian distribution on a sphere and is parameterized by only a few variables - principal direction and a concentration parameter.

2.1. Paired von Mises-Fisher Distribution

In its most general form, von Mises distribution [23], generalized to a hyper-sphere, S_{p-1} , is given as

$$M_p(\mathbf{x}; \boldsymbol{\mu}, \kappa) = \left(\frac{\kappa}{2}\right)^{p/2-1} \frac{1}{\Gamma(p/2)I_{p/2-1}(\kappa)} \exp(\kappa \boldsymbol{\mu}^T \mathbf{x}). \quad (1)$$

where $\kappa \geq 0$ is the concentration parameter, $\boldsymbol{\mu}$, (with $\|\boldsymbol{\mu}\| = 1$) is the principal direction and I_ν is the Bessel function of the first kind and order ν . The concentration parameter κ indicates the concentration of the function around the mean direction $\boldsymbol{\mu}$. For the 3 dimensional case, which is of our immediate interest, this distribution is called von Mises-Fisher distribution and has the form

$$M_3(\mathbf{x}; \boldsymbol{\mu}, \kappa) = \frac{\kappa}{4\pi \sinh \kappa} \exp(\kappa \boldsymbol{\mu}^T \mathbf{x}). \quad (2)$$

At this point we note that as the data we are dealing with is antipodally symmetric, it can be more succinctly described by an axial distribution. This can be easily achieved by pairing each von Mises-Fisher distribution with its antipodal counterpart. This translates to assigning to each direction, μ , a distribution which is an average of two von Mises-Fisher distributions which are oriented along the mean directions μ and $-\mu$. Expression for such a paired von Mises-Fisher distribution is given by

$$\tilde{M}_3(\pm\mathbf{x}; \boldsymbol{\mu}, \kappa) = \frac{\kappa}{4\pi \sinh \kappa} \cosh(\kappa \boldsymbol{\mu}^T \mathbf{x}). \quad (3)$$

An advantage of using this form for the paired von Mises-Fisher distribution is that the integrations involving this distribution can still be carried out over the sphere.

2.2. Continuous Mixture of Paired von Mises-Fisher Distributions

Generalizing the concept of discrete mixture of distributions, we propose to use a continuous mixture of the paired von Mises-Fisher distributions (Eq. 3) to model the MR signal. If we assume the existence of a density function $f(\boldsymbol{\mu})$ with respect to a probability measure, $d\boldsymbol{\mu}$, associated with each direction on a sphere, we can define the continuous mixture of paired von Mises-Fisher distributions as

$$B(\pm\mathbf{x}; \kappa) = \int_{S^2} f(\boldsymbol{\mu}) \tilde{M}_3(\pm\mathbf{x}; \boldsymbol{\mu}, \kappa') d\boldsymbol{\mu}. \quad (4)$$

According to the unified de-convolution framework presented by Jian et al. [18], in our model $\tilde{M}_3(\pm\mathbf{x}; \boldsymbol{\mu}, \kappa')$ is the convolution kernel function and $f(\boldsymbol{\mu})$ is the mixing density. The mixing density is useful in handling the intra-voxel orientational heterogeneity as it gives a continuous representation of the contributing volume fractions. In the literature, various proposals have been made to pick the kernel and the mixing density functions (e.g. [1], [4]). For our choice of kernel function defined in eq. 3, we again pick the von Mises-Fisher (eq. 2) as the mixing density. Our reason for picking the von Mises-Fisher density as the mixing density is two-fold. Firstly, it is a common practice to put an analog of the Gaussian distribution as the prior on the kernel variable distribution (e.g. Jian et al. [19] use the Wishart distribution as prior on concentration matrix distribution because it the analog of Gaussian distribution on P_n , the manifold of symmetric positive definite matrices). By the same token, von Mises-Fisher is the analog of Gaussian distribution on S^2 , the manifold of orientations. Secondly and more importantly, using a von Mises-Fisher density leads to a closed form expression for the diffusion weighted MR signal.

Now we make the important observation that a single von Mises-Fisher as the mixing density would not be able to accurately resolve the intra-voxel fiber orientational heterogeneity as it a unimodal density and convolution of

two unimodal functions leads back to a unimodal function. Therefore, we propose the use of a discrete mixture of von Mises-Fisher distributions for the mixing density as $\sum_{i=1}^N w_i M_3(\mathbf{x}; \boldsymbol{\mu}_i, \kappa)$. It must be noted that (also pointed out in [19] and [18]) N is only the resolution of the discretization of the manifold S_2 and should not interpreted as the number of expected fiber bundles. It can also be looked as the number of basis function that are to be used to reconstruct the MR signal (more the number of basis functions, better the reconstruction). Finally, we note that substituting the expression for the mixing density in eq. 4 and setting convolution kernel function parameter $\kappa' = 1$, leads to an expression which can be interpreted as the Laplace transforms of a mixture of von Mises-Fisher distributions, which we have analytically computed and thus our model for the MR signal is

$$S(\mathbf{q})/S_0 = \sum_{i=0}^N w_i \frac{\kappa}{4\pi \sinh(1) \sinh \kappa} \left[\frac{\sinh(\|\kappa \boldsymbol{\mu}_i - \mathbf{q}\|)}{\|\kappa \boldsymbol{\mu}_i - \mathbf{q}\|} + \frac{\sinh(\|\kappa \boldsymbol{\mu}_i + \mathbf{q}\|)}{\|\kappa \boldsymbol{\mu}_i + \mathbf{q}\|} \right], \quad (5)$$

where $S(\mathbf{q})$ is the observed signal, S_0 is the signal in absence if diffusion weighting gradient and \mathbf{q} encodes the magnitude and the direction of the diffusion sensitizing gradients. The advantage of having the closed analytical form in eq. 5 is that the unknown weights w_i can be obtained readily by solving a linear system $Aw = s$ where

$$A_{j,i} = \frac{\kappa}{4\pi \sinh(1) \sinh \kappa} \left[\frac{\sinh(\|\kappa \boldsymbol{\mu}_i - \mathbf{q}_j\|)}{\|\kappa \boldsymbol{\mu}_i - \mathbf{q}_j\|} + \frac{\sinh(\|\kappa \boldsymbol{\mu}_i + \mathbf{q}_j\|)}{\|\kappa \boldsymbol{\mu}_i + \mathbf{q}_j\|} \right], \quad (6)$$

w is the vector of unknown weights and s is the vector obtained by stacking $S(\mathbf{q}_j)/S_0$. Note that \mathbf{q}_j are the various directions in which gradient is applied to obtain the MR reading. We obtain the least square solution for this linear system using pseudoinverse.

Here we must point two important differences between our model and the mixture of Wisharts (MoW) model proposed by Jian et al. ([19],[17]). Firstly, MoW makes the simplifying assumptions that the diffusion tensor has fixed eigenvalues. This is required because P_n , the manifold of symmetric positive definite matrices, cannot be discretized but fixing the eigenvalues translates that problem to discretizing the manifold of orientations, S_2 , which is not a problem. In our model no such simplifying assumption is required as we work directly with a distribution defined on S_2 . Secondly, MoW method requires that the mixture

has sparse and positive weights which necessitates the use of an iterative algorithm like Non-Negative Least Squares (NNLS) [21]. In our method, since we look at the columns of matrix A as basis set for the MR signal reconstruction, we allow negative weights and thus computationally light pseudoinverse solution works well. Another major advantage of pseudoinverse solution is that pseudoinverse need be computed only once. We must point out that no significant distortion due to possible ill-conditioning of A matrix was observed (as indicated by the experimental results).

2.3. Fiber Orientation Recovery

Once the MR signal has been reconstructed, the relation of the water displacement probability to MR signal is given through a Fourier transform as

$$P(r_0\mathbf{r}) = \int \frac{S(\mathbf{q})}{S_0} e^{-2\pi i \mathbf{q}^T \mathbf{r} r_0} d\mathbf{q}, \quad (7)$$

where \mathbf{q} is the reciprocal space vector, $S(\mathbf{q})$ is the DW-MRI signal value associated with vector \mathbf{q} , S_0 the zero gradient signal and \mathbf{r} and r_0 is the direction and magnitude respectively of the displacement vector [12].

There are various approaches for computing $P(r_0\mathbf{r})$. MR signal $S(\mathbf{q})$ can either be first reconstructed and then Eq. 7 be evaluated ([17]) or the displacement probability can be directly computed from the given diffusion-weighted MR data ([26]). Yet another technique seeks an alternative representation called the fiber orientation distribution (from the Q-Ball images) from which the optimal fiber orientations can be derived ([13], [4]). In this work we used the method proposed in [7], though any of the above mentioned methods would also work.

Once the water displacement probability has been estimated, orientations of the underlying distinct fiber bundles can be recovered using the spherical function $p(\mathbf{r})$ which is extracted from the volume of $P(r_0\mathbf{r})$ by either fixing r_0 ([26]) or by integrating over r_0 ([36]) and then finding the maxima of $p(\mathbf{r})$. In this work we follow the former of these two approaches to recover the final fiber orientations.

3. Experimental Results

In this section we present various experimental results obtained by applying our method to synthetic as well as real diffusion weighted MR data from excised, perfusion-fixed rat optic chiasm and rat brain datasets. In all our experiments we constructed the proposed basis $A_{j,i}$ (given by Eq. 6) by discretizing the space of unit vectors μ_i using a 4th order subdivision of the icosahedral tessellation of the unit hemi-sphere.

Figure 1 shows spherical plots of the von Mises-Fisher distribution (upper row), the paired von Mises-Fisher (middle row) and the corresponding proposed basis (lower row)

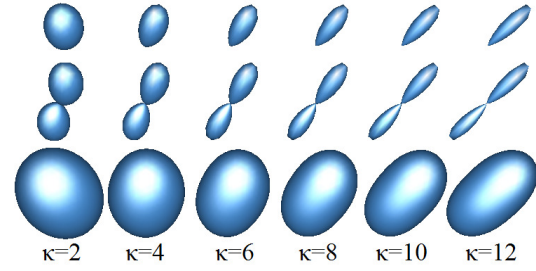


Figure 1. Upper row: Visualization of the von Mises-Fisher distribution (Eq. 2) for various values of κ . Middle row: The paired von Mises-Fisher distribution. Lower row: The corresponding proposed basis functions (column of matrix A (Eq. 6)) plotted as spherical functions (i.e. for all unit vectors \mathbf{q}_j).

for different values of the parameter κ . It can be noted that different choices of κ does not alter the shape of the obtained basis significantly (see Fig. 1 bottom row). This was also noted by us in our experiments with synthetic and real data and thus for the rest of section, we assume the value of κ to be fixed to 10.

In order to compare the performance of the proposed model with other existing state-of-the-art methods, we conducted experiments on synthesized two fiber crossing DW-MRI data with known fiber directions (so that errors could be computed). The dataset was generated by simulating the diffusion-weighted MR signal attenuation using the model proposed in [29]. The signal was simulated for 81 magnetic gradient directions with the b-value = 1250s/mm². In order to test the performance of the models under varying noise conditions, different amounts of Riccian noise was added to the data (standard deviation 0.02 to 0.14). The noise corrupted data was then used for signal reconstruction using the diffusion orientation transformation (DOT) [26] method, the ODF method proposed in [14], the fourth order tensor model (DT4) [6], the continuous mixture of Wishart distributions (MOW) [17] and the proposed continuous mixture of von Mises-Fisher (MOVIM). To quantitatively compare the performance of our method with other methods, the fiber orientation errors were estimated for all the methods. This experiment was repeated 100 times and the mean and standard deviation of the fiber orientation errors are presented in Fig. 2.

It can be noted in Fig. 2 that the proposed method performs significantly better than the DOT, ODF and DT4 models especially in the higher noise cases. Furthermore, the performance of the proposed model is generally similar to that of MOW, especially in the typical case of noise with signal to noise ratio (SNR): 12.5 – 16.6. In addition to the quantitative error measurements, the displacement probability profiles recovered by our method (MOVIM) using data

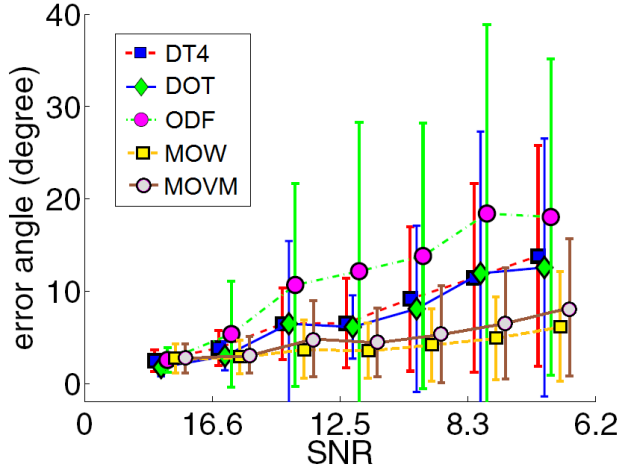


Figure 2. Plot of the mean and standard deviation of the fiber orientation error (in degrees) estimated using the methods: DOT [26], ODF [14], DT4 [6], MOW [17] and the proposed MOVm.

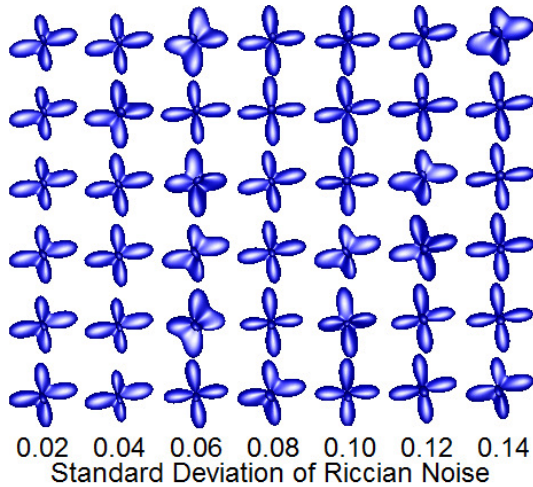


Figure 3. The displacement probability profiles corresponding to the signal reconstructed by the proposed method using data corrupted with varying amount of noise.

corrupted with varying amount of noise is presented in Fig. 3 for visual inspection. These last two experiments validate the accuracy of our model in estimating multiple fiber orientations and demonstrate its robustness in presence of high levels of noise in the data.

Next, we show results for application of our method to a real diffusion-weighted MR data set obtained from an excised perfusion-fixed rat brain. The data collection protocol included acquisition of 32 images using a spin-echo, pulsed-field-gradient sequence with repetition time 1.4 s, echo time 28 ms, field-of-view 30 mm \times 15 mm, matrix 200 \times 100 with 32 continuous 0.3-mm-thick slices measured (oriented parallel to the long-axis of the brain). 46

diffusion-weighted images were collected with 5 signal averages with approximate b values of 1250 s/mm², whose orientations were determined by the tessellation on a hemisphere.

Figure 4 depicts a region of interest (ROI) showing fibers of cingulum and corpus callosum intersecting each other. On the lower left corner in this figure the zero gradient image S_0 is shown. The square box indicates the ROI which is presented enlarged in the rest of the image. The displacement probability iso-surface estimated from the reconstructed signal by the proposed method is shown within each voxel. Each probability iso-surface is colored according to its dominant fiber direction. The colormap mapping the directions to the colors is shown on the upper left corner of the figure (same color coding is used in the next two figures). In the upper right side of the ROI, single fiber structures that correspond to the fibers from corpus callosum are shown to be correctly estimated. At the center of the ROI, where a number of fibers intersect, the proposed method estimated fiber crossings and other complex fiber structures, which demonstrates the effectiveness of the proposed model.

Figure 5 shows the region containing the hippocampus from the same data set. As before, the rectangular box in the S_0 image (lower left) indicates the ROI which is shown zoomed in the rest of the figure. The estimated structures include fiber crossings and single fibers which are consistent to other published studies on the structure of hippocampus [28, 3].

We also applied our model to a set of diffusion-weighted MR data taken from excised, perfusion-fixed rat optic chiasm [26](46 diffusion gradient directions, b-value \approx 1250 s/mm²). Figure 6 shows the probability profiles computed from the reconstructed signal. The rectangular box in the S_0 image (lower left) indicates the ROI which shows myelinated axons from the two optic nerves crossing each other to reach their respective contra-lateral optic tracts. The probability profiles computed by our method brings out this expected behavior of the fiber structures. These recovered fiber structures are consistent with other studies on this anatomical region of the rat nervous system [26].

4. Conclusion

In this paper, we introduce a novel mathematical model for estimating the MR signal using a continuous mixture of von Mises-Fisher distributions. Since the von Mises-Fisher distributions are defined on sphere, simplifying assumptions to transform the discretization problem from the space of symmetric positive definite matrices ([19], [17]) to the sphere are not required. Further, our technique leads to a linear system which does not require a sparse solution and thus produces good results even with computationally light pseudoinverse solution. Through experimentation

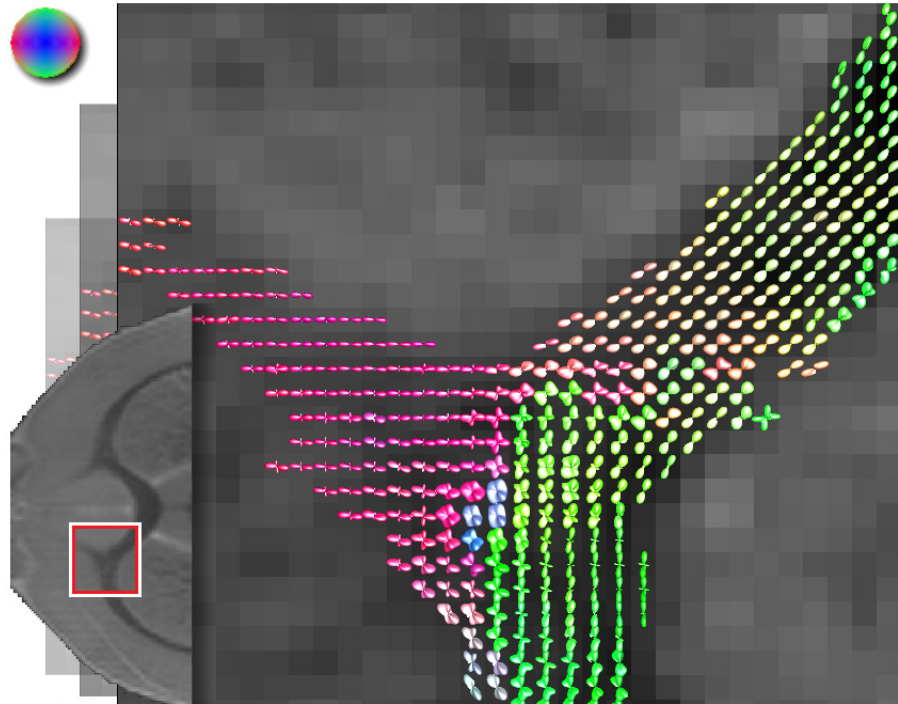


Figure 4. Real DW-MRI data from a rat brain. The figure shows displacement probability iso-surfaces estimated from the reconstructed signal by the proposed method. The depicted ROI shows intersecting fibers from cingulum and corpus callosum.

on benchmark synthetic data for fiber crossing we demonstrate that our method performs better than most state-of-the-art techniques and similar to MoW. Further, to validate the applicability of this method to real data, we present the recovered fiber orientations for rat brain and optic chiasm datasets. From our results on synthetic and real data it can be concluded that the performance of our novel method is comparable, if not better than the state-of-the-art in DW-MRI image analysis.

References

- [1] D. C. Alexander. Maximum entropy spherical deconvolution for diffusion MRI. In *IPMI*, pages 76–87, 2005.
- [2] D. C. Alexander, G. J. Barker, and S. R. Arridge. Detection and modeling of non-Gaussian apparent diffusion coefficient profiles in human brain data. *Magn. Reson. Med.*, 48(2):331–340, August 2002.
- [3] D. Amaral and M. Witter. Hippocampal formation. In *The Rat Nervous System*, pages 443–493. Academic Press, 1995.
- [4] A. W. Anderson. Measurement of fiber orientation distributions using high angular resolution diffusion imaging. *Magn. Reson. Med.*, 54(5):1194–1206, 2005.
- [5] Y. Assaf, R. Z. Freidlin, G. K. Rohde, and P. J. Basser. New modeling and experimental framework to characterize hindered and restricted water diffusion in brain white matter. *Magn. Reson. Med.*, 52(5):965–978, 2004.
- [6] A. Barmpoutis, B. Jian, B. C. Vemuri, and T. M. Shepherd. Symmetric positive 4th order tensors and their estimation from diffusion weighted MRI. In *IPMI*, pages 308–319, 2007.
- [7] A. Barmpoutis, B. C. Vemuri, and J. R. Forder. Fast displacement probability profile approximation from hardi using 4th-order tensors. In *ISBI*, 2008.
- [8] P. J. Basser, J. Mattiello, and D. Lebihan. Estimation of the Effective Self-Diffusion Tensor from the NMR Spin Echo. *J. Magn. Reson. B.*, 103:247–254, 1994.
- [9] T. Behrens, H. Johansen-Berg, S. Jbabdi, M. Rushworth, and M. Woolrich. Probabilistic tractography with multiple fibre orientations: What can we gain? *NeuroImage*, 34:144–155, 2007.
- [10] T. Behrens, M. Woolrich, M. Jenkinson, H. Johansen-Berg, R. Nunes, S. Clare, P. Matthews, J. Brady, and S. Smith. Characterization and propagation of uncertainty in diffusion-weighted mr imaging. *Magn. Reson. Med.*, 50(2):1077–1088, 2003.

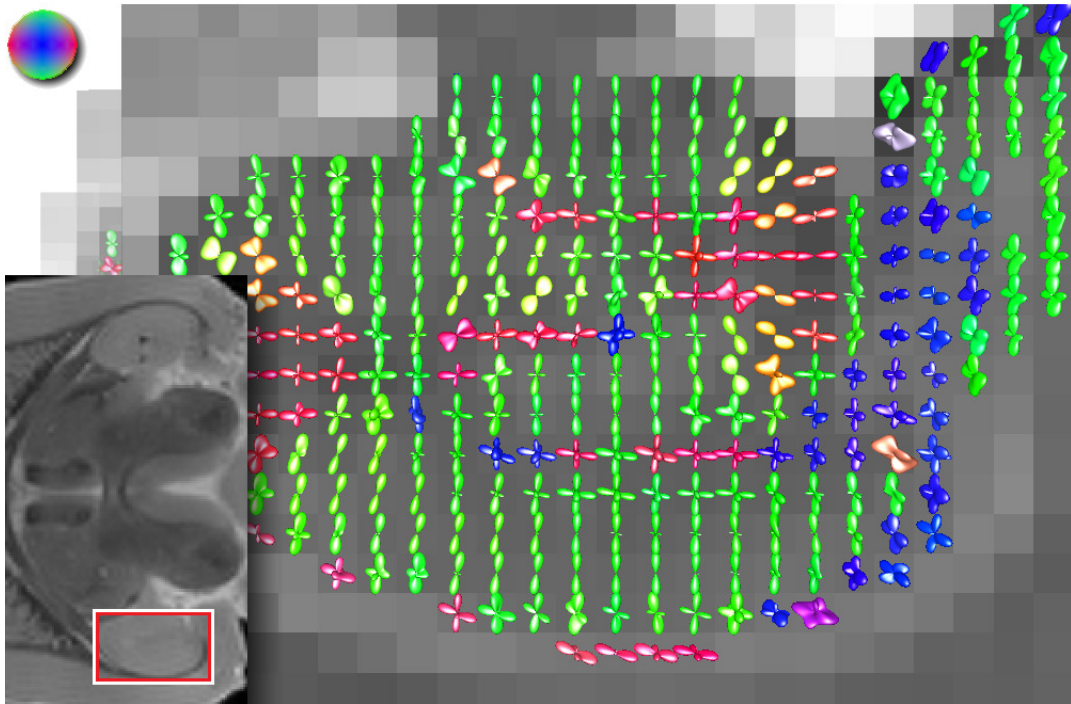


Figure 5. Real DW-MRI data from a rat brain. The ROI contains the hippocampus where various fiber structures estimated by the proposed method can be seen.

- [11] A. Bhalerao and C.-F. Westin. Hyperspherical von mises-fisher mixture (hvmf) modelling of high angular resolution diffusion mri. *Medical Image Computing and Computer-Assisted Intervention MICCAI 2007*, pages 236–243, 2007.
- [12] P. T. Callaghan. *Principles of Nuclear Magnetic Resonance Microscopy*. Clarendon Press, Oxford, 1991.
- [13] R. Deriche and M. Descoteaux. Splitting tracking through crossing fibers: Multidirectional q-ball tracking. *ISBI*, pages 756–759, 2007.
- [14] E. Descoteaux, E. Angelino, S. Fitzgibbons, and R. Deriche. A fast and robust odF estimation algorithm in q-ball imaging. *ISBI: From Nano to Macro*, 2006.
- [15] L. R. Frank. Characterization of anisotropy in high angular resolution diffusion-weighted MRI. *Magn Reson Med*, 47(6):1083–1099, 2002.
- [16] C. P. Hess, P. Mukherjee, E. T. Han, D. Xu, and D. B. Vigneron. Q-ball reconstruction of multimodal fiber orientations using the spherical harmonic basis. *Magn. Reson. Med.*, 56(1):104–117, 2006.
- [17] B. Jian and B. C. Vemuri. Multi-fiber reconstruction from diffusion MRI using mixture of Wisharts and sparse deconvolution. In *IPMI*, pages 384–395, 2007.
- [18] B. Jian and B. C. Vemuri. A unified computational framework for deconvolution to reconstruct multiple fibers from diffusion weighted MRI. *IEEE Transactions on Medical Imaging*, 26(11):1464–1471, 2007.
- [19] B. Jian, B. C. Vemuri, E. Özarslan, P. R. Carney, and T. H. Mareci. A novel tensor distribution model for the diffusion weighted MR signal. *NeuroImage*, 37(1):164–176, 2007.
- [20] M. Köpf, R. Metzler, O. Haferkamp, and T. F. Nonnenmacher. NMR studies of anomalous diffusion in biological tissues: Experimental observation of Lévy stable processes. In G. A. Losa, D. Merlini, T. F. Nonnenmacher, and E. R. Weibel, editors, *Fractals in Biology and Medicine*, volume 2, pages 354–364. Birkhäuser, Basel, 1998.
- [21] C. Lawson and R. J. Hanson. *Solving Least Squares Problems*. Prentice-Hall, 1974.
- [22] M. Lazar, D. M. Weinstein, J. S. Tsuruda, K. M. Hasan, konstantinos Arfanakis, E. M. Meyerand, B. Badie, H. A. Rowley, V. Haughton, A. Field, and A. L. Alexander. White matter tractography using diffusion tensor deflection. *Human Brain Mapping*, 18(4):306–321, 2003.
- [23] K. V. Mardia and P. Jupp. *Directional Statistics*. John Wiley and Sons Ltd., Newyork, 2nd Edition, 2000.
- [24] T. E. McGraw, B. C. Vemuri, R. Yeziarski, and T. H. Mareci. Von Mises-Fisher mixture model of the diffusion ODF. In *Proceedings of IEEE International Symposium on Biomed-*

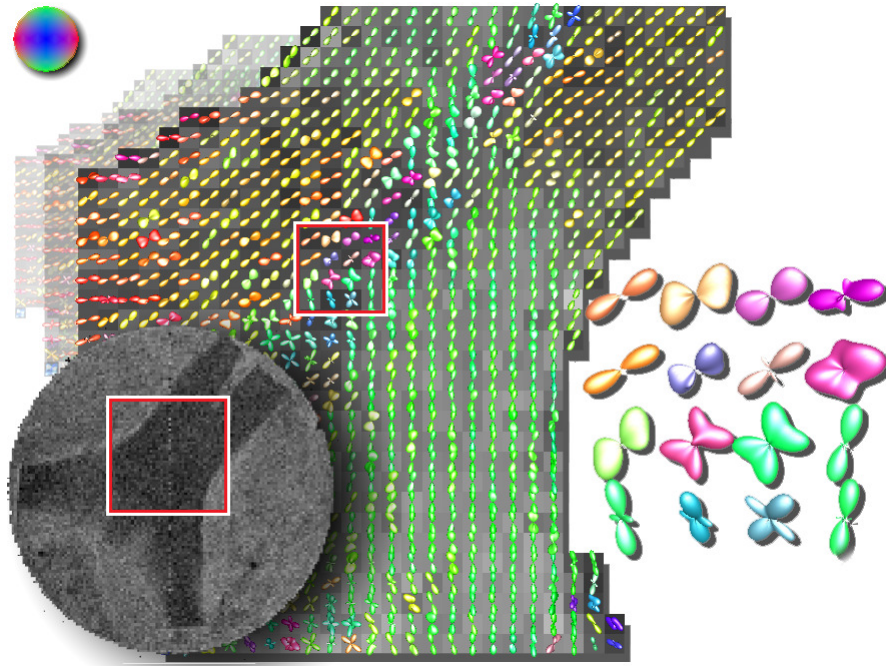


Figure 6. Real DW-MRI data showing a rat's optic chiasm. The zoomed-in ROI shows estimated crossings in the central region of the optic chiasm where the two optic nerves from the contra-lateral parts of the brain cross each other.

- ical Imaging: From Nano to Macro (ISBI)*, pages 65–68, 2006.
- [25] E. Özarslan and T. H. Mareci. Generalized diffusion tensor imaging and analytical relationships between diffusion tensor imaging and high angular resolution diffusion imaging. *Magn. Reson. Med.*, 50(5):955–965, 2003.
- [26] E. Özarslan, T. M. Shepherd, B. C. Vemuri, S. J. Blackband, and T. H. Mareci. Resolution of complex tissue microarchitecture using the diffusion orientation transform (DOT). *NeuroImage*, 31:1086–1103, 2006.
- [27] J. P. Rigaut. An empirical formulation relating boundary lengths to resolution in specimens showing non-ideally fractal dimensions. *J Microsc.*, 133:41–54, 1984.
- [28] T. M. Shepherd, E. Özarslan, M. A. King, T. H. Mareci, and S. J. Blackband. Structural insights from high-resolution diffusion tensor imaging and tractography of the isolated rat hippocampus. *NeuroImage*, 32(4):1499–1509, 2006.
- [29] O. Söderman and B. Jönsson. Restricted diffusion in cylindrical geometry. *J. Magn. Reson. B*, 117(1):94–97, 1995.
- [30] E. O. Stejskal and J. E. Tanner. Spin diffusion measurements: Spin echoes in the presence of a time-dependent field gradient.
- [31] J.-D. Tournier, F. Calamante, D. G. Gadian, and A. Connelly. Direct estimation of the fiber orientation density function from diffusion-weighted MRI data using spherical deconvolution. *NeuroImage*, 23(3):1176–1185, November 2004.
- [32] J.-D. Tournier, F. Calamante, and A. Connelly. Improved characterisation of crossing fibres: spherical deconvolution combined with Tikhonov regularization. In *Proceedings of the ISMRM 14th Scientific Meeting and Exhibition*, Seattle, Washington, 2006.
- [33] D. S. Tuch. *Diffusion MRI of Complex Tissue Structure*. PhD thesis, MIT, 2002.
- [34] D. S. Tuch. Q-ball imaging. *Magn. Reson. Med.*, 52(6):1358–1372, 2004.
- [35] D. S. Tuch, T. G. Reese, M. R. Wiegell, N. Makris, J. W. Belliveau, and V. J. Wedeen. High angular resolution diffusion imaging reveals intravoxel white matter fiber heterogeneity. *Magn. Reson. Med.*, 48(4):577–582, 2002.
- [36] D. S. Tuch et al. Diffusion MRI of complex neural architecture. *Neuron*, (40):885–895, 2003.
- [37] V. J. Wedeen, P. Hagmann, W.-Y. I. Tseng, T. G. Reese, and R. M. Weisskoff. Mapping complex tissue architecture with diffusion spectrum magnetic resonance imaging. *Magn. Reson. Med.*, 54(6):1377–1386, 2005.
- [38] J. Weickert and H. Hagen, editors. *Visualization and Processing of Tensor Fields*. Springer, 2005.